infrastructures

MDPI

Article

Evaluating the Performance of Lateritic Soil Stabilized with Cement and Biomass Bottom Ash for Use as Pavement Materials

Arsit Iyaruk, Panu Promputthangkoon and Arun Lukjan *

Department of Civil Engineering, Rajamangala University of Technology Srivijaya, Songkhla 90000, Thailand; arsit.i@rmutsv.ac.th (A.I.); panu.p@rmutsv.ac.th (P.P.)
* Correspondence: arun.l@rmutsv.ac.th

Abstract: From the perspective of sustainable waste management and its environmental impact, waste biomass bottom ash (BA) remains problematic and challenging to use as a recycling material for civil engineering infrastructures. This study evaluated the performance of lateritic soil (LS), stabilized with cement and biomass BA, as a subbase material. BA has been considered a replacement material in LS prior to the introduction of hydraulic cement stabilization means. The geotechnical engineering tests comprised the modified Proctor test, the California Bearing Ratio (CBR) test, and the unconfined compression test. X-ray fluorescence (XRF) and X-ray diffraction (XRD) tests were conducted to investigate the mineralogical properties of the stabilized soil samples. The leachate test was performed with a permeability mold to measure the release of heavy metals. Finally, the benefits of using the stabilized subbase material were assessed using the mechanistic–empirical (M–E) pavement design approach. Based on the results obtained, the strength and stiffness characteristics of the stabilized soils indicate that the efficiency of the mix satisfied the Thailand highway specification. The admixture of 80% BA and 5% cement is suggested for use as a soil–cement subbase material for flexible pavements, due to its good engineering and environmental properties. The results of the M–E design demonstrate the effectiveness of the stabilized soil presented herein. The study's outcomes are predicted to promote the utilization of waste BA as a promising pavement material.

Keywords: bottom ash; hydraulic cement; stabilization; mechanistic–empirical; traffic benefit ratio

Citation: Iyaruk, A.; Promputthangkoon, P.; Lukjan, A. Evaluating the Performance of Lateritic Soil Stabilized with Cement and Biomass Bottom Ash for Use as Pavement Materials. *Infrastructures* **2022**, *7*, 66. https://doi.org/10.3390/infrastructures7050066

Academic Editor: Víctor Yepes

Received: 9 April 2022
Accepted: 26 April 2022
Published: 29 April 2022

1. Introduction

Transportation infrastructure has increasing demands due to the increasing population, and rapid growth of the economy, society, and industry. Thailand has a long-term plan for the development of the overall transportation infrastructure, especially road transportation, which is the most popular means of transport in Thailand [1]. Lateritic soil (LS) is generally used as road material—for example, in subbase layers in Thailand, and in other tropical regions (Malaysia, Brazil, Nigeria, etc.). However, the majority of the remaining tropical lateritic soil contains a large percentage of fine-grained soil particles, resulting in poor engineering properties. Moreover, it is well known that the engineering characteristics of weathered lateritic soil from different sources differ depending on their chemical and physical processing. As a result, approaches to improve the characteristics of certain types of soils as road materials are required [2].

Soils in tropical and arid areas are always unsaturated due to climatic conditions. The key feature of the unsaturated zone is the negative pore-water pressure or suction, which varies with soil moisture content. As a result of variable moisture content, soil properties are relatively constant in the saturated zone but vary spatially and temporally in the unsaturated zone. In general, ignoring unsaturated effects increases the safety of the geo-structure design. The suction profile beneath a covered ground surface is more constant over time than the profile beneath an uncovered surface. However, moisture may slowly accumulate below the covered area over time, causing a reduction in soil

suction. As the flexible pavement is covered by an asphalt concrete layer, it helps to prevent water infiltration into the pavement structure. In this case, the soil suction profile remains relatively constant throughout the dry and wet seasons [3]. Therefore, the effects of unsaturated soils on the strength characteristics and performance were unconsidered in this study.

Waste industrial recycling and management is still a broad concern in civil engineering works to help to reduce the impacts of environmental hazards caused by waste disposal (plastic, rubber tire, fly ash, bottom ash, etc.). The focus of this paper is biomass bottom ash. Biomass ashes (i.e., fly ash and bottom ash) are by-products of biomass combustion, which is considered a clean energy source with no CO_2 emissions [4]. This industrial waste ash is highly recyclable, resulting in economic and environmental benefits. Bottom ash, which has higher strength and less heavy metal leaching than fly ash, can be used in all highway material layers [5]. The positive results of this waste ash utilization in road construction applications can be found in numerous previous works. For instance, López et al. [6] characterized two types of silica–aluminous bottom ashes in Spain, and suggested that soils can be improved by incorporating bottom ash contents ranging from 15 to 40% of the soil's weight, thereby increasing their load-bearing capacity while decreasing their plasticity. Cabrera et al. [7] investigated the feasibility of using biomass bottom ash (BA) across three different power plants in Spain's civil infrastructure environment, based on their physicochemical properties. They suggested that restricting the level of organic matter in the BA would allow it to be used as a filler material for embankments and a broader range of civil infrastructures.

Regarding with leaching of some heavy metals in the biomass ashes, pretreatment methods (separation, solidification/stabilization (S/S), heat treatment, etc.) are required [5]. Chemically treated soils are a common technique in road construction, alongside typical additives, such as fly ash, cement, and lime. Cement-based stabilization techniques are widely used as stabilized materials in pavement structure layers, for instance, in the study by [8–11]. The use of incinerator bottom ash (IBA) as cement-bound material for use as road material in the UK was reported by Paine et al. [8]. The authors suggested that the IBA can be practically used in proportions of 40% or more by mass of aggregate with a cement content of about 2–8%, which met the compressive strength of UK highway specifications and is well within typical regulatory drinking limits. Jaritngam et al. [9] concluded that approximately 3% Portland cement is sufficient to stabilize lateritic soil for use as a road base material that meets Thailand Department of Highways (DOH) specifications and can be a cost-effective substitute for crushed rock. While Donrak et al. [11] reported that using 5% cement-stabilized lateritic soil and melamine debris blends as subbase materials can be used safely in sustainable pavement applications.

A mechanical and durability investigation of cement-treated lateritic soil in Malaysia was carried out by Wahab et al. [12]. The study results indicated that the strength development of 9 and 12% cement-treated lateritic specimens showed an increasing trend against wet-dry cycles, which led to long-term pozzolanic reactions. The leaching potential of the material usually has been determining the acceptance criteria for reusing bottom ash in road applications, in both laboratory (e.g., [8,13]) and field performance (e.g., [14–16]) investigations. Del Valle-Zermeno et al. [17] built a pilot-scale road subbase made with granular material stabilized with bottom ash and cement mortar in Spain. The results revealed that the pozzolanic effect of the cement mortar is responsible for the immobilization of all heavy metals. Cabrera et al. [18] investigated the leaching behavior of 5% cement-treated recycled aggregate and BA mixtures using a standard column test. They claimed that the use of BA in road construction had no negative effects on the environment.

Numerous researchers have performed laboratory testing of chemically treated soils, followed by performance analysis using numerical modeling, to assess the feasible use of waste materials due to the limitation of full-scale tests of roads. The basic idea behind using mechanistic modeling techniques for pavement design is to choose the thickness of the pavement structure which will limit the vertical compressive strains at the top of the

subgrade, and the horizontal tensile strains at the bottom of the asphalt surface caused by traffic loads [19]. Lekha et al. [20] reported on the strength and durability improvements in lateritic soil stabilization with 1% Arecanut coir and 3% cement. They found that the stress and displacement of the pavement structure were reduced by 6–10% and 4–18% respectively, when using the KENLAYER (The University of Kentucky, Lexington, KY, USA) computer program. Stabilizing fly ash and lime sludge mixed with lime and gypsum for use as a road construction material was explored by Sahu et al. [21]. The three-layered flexible pavement was built using the finite element code PLAXIS 2D, including a reliability index for rutting and fatigue failure of the pavement. The authors suggested that the study outcome is useful for assessing the performance of the pavement concerning rutting and fatigue failure under a given environment. Anaokar and Mhaiskar [22] investigated the effectiveness of a C-shaped lime-stabilized capping beneath an embankment carrying flexible pavement on an expansive subgrade. PLAXIS 3D (Bentley Systems, Exton, PA, USA) was used to investigate load displacement behaviors. The authors concluded that lime-stabilized capping, consisting of a horizontal buffer layer and vertical cut-offs, was effective at controlling swelling displacements in expansive subgrades. Other studies also used mechanistic modeling techniques; for example, the finite element method PLAXIS 2D to investigate the displacement behavior of the coal gangue embankment in China [23], and KENLEYER software to evaluate the performance of using cement-stabilized soil for the flexible pavement in China [24] and the USA [25–27]. These studies have shown the effectiveness of using the M–E method in pavement design, providing important results for the assessment of the proposed materials.

Ordinary Portland cement (OPC) is a traditional cementitious material for road applications with a cement content of 2 to 10% (e.g., [9,11,12,28]). However, cement production accounts for approximately 5–8% of total anthropogenic CO_2 emissions, owing primarily to the conversion of $CaCO_3$ into CaO, and the combustion of fossil fuels during the mixing of raw materials during heating [29,30]. Many efforts have been made to reduce these emissions, including the use of alternative cementitious materials such as blast furnace slags and fly ash from coal combustion in the place of traditional Portland cement [29]. Hydraulic cement (HC) is an inorganic material that, when mixed with water, hardens and becomes water-resistant [30]. HC consists of about 10% clinker-replacement materials (calcium carbonate, limestone, fly ash, natural pozzolan, etc.). In the studies mentioned, none utilized environment-friendly cementitious materials such as HC for road pavement applications. Furthermore, biomass waste is widely used as a biofuel for power generation in Thailand. The seven biomass combustion plants provide approximately 60 MW of electrical energy capacity (23,000 toes) to the Songkhla Province, which is regarded as the economic center in the lower part of southern Thailand. A report by the Songkhla Provincial Industry, there are issues with waste ash management due to large amounts of biomass ash (i.e., fly ash and bottom ash), which makes it difficult to develop the industrial area into an eco-industrial town [31].

Therefore, this study evaluates the feasibility and performance of utilizing local LS mixed with BA and HC mixtures as soil–cement subbase materials. Three main tasks were carried out—namely: (1) geotechnical engineering tests to analyze the strength development; (2) laboratory leaching tests for the estimation of potential heavy metal release; (3) pavement design and analysis of the pavement's life using the mechanistic–empirical approach. Based on the results obtained, the feasibility of BA in civil infrastructures is then presented. Additionally, the work presented in this paper could contribute substantially to the reduction of greenhouse gas emissions from cement production. The replacement of biomass ash in the soil–cement subbase would result in additional benefits toward reducing the consumption of energy and raw materials in the cement industry, besides also reducing the direct impact of landfills associated with biomass combustion residues.

2. Materials and Methods

2.1. Materials

2.1.1. Lateritic Soil

Samples of lateritic soil (LS) used in this study were collected from the local borrow pit site of the Hat Yai Sub-district, Songkhla Province. The LS sample was tested to define its physical properties, which comprised wet sieve analysis, specific gravity, and Atterberg's limit tests. The results of the soil characterization tests are summarized in Table 1. As observed in Table 1, the LS consisted of 32% gravel, 21% sand, and 47% fine-grained soil. The particle size distribution of the soil is shown in Figure 1. The median particle size (D_{50}) of soil was 0.15 mm, and the specific gravity was 2.755. The soil consistency parameters were 30, 21, and 9% for the liquid limit (LL), plastic limit (PL), and plasticity index (PI), respectively. According to the Unified Soil Classification System (USCS), the lateritic soil sample was classified as reddish–yellow clayey gravel with sand (GC). The LS had a wearing resistance value of more than 60% based on the Los Angeles abrasion test, which did not meet the subbase specification of the Department of Highways (DOH) of Thailand [32].

Table 1. Physical properties of the LS and BA.

Materials	Specific Gravity	Consistency Limit (%)			D_{50} (mm)	Soil Fraction (%)			USCS Symbol
		LL	PL	PI		Gravel	Sand	Silt & Clay	
LS	2.755	30	21	9	0.15	32	21	47	GC
BA	2.405	Non-plastic			1.60	26	71	3	SP

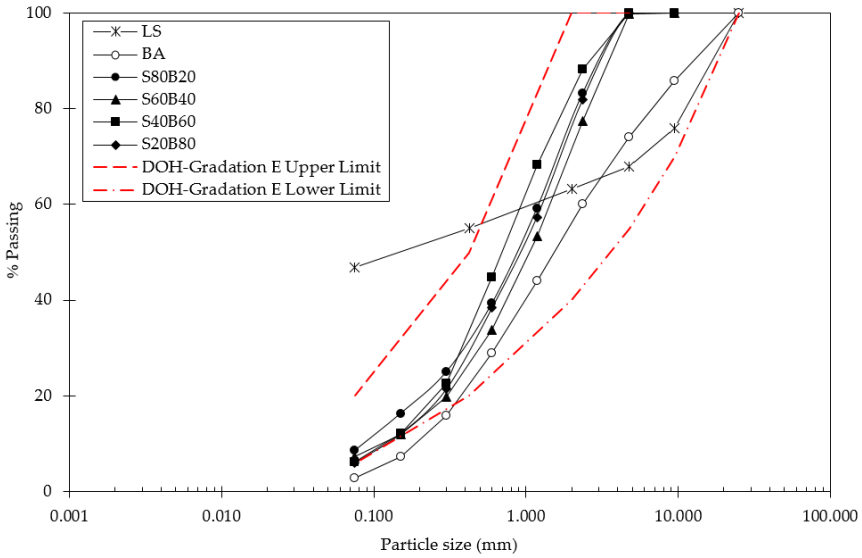

Figure 1. Grain size distribution curves of the LS, BA, and LS+BA.

The chemical composition of the LS from the X-ray fluorescence (XRF) test is presented in Table 2. The dominant compounds in the soil were silicon dioxide (59.79%), aluminum oxide (20.59%), and ferric oxide (8.07%). The total amount of major components of 88.44% can be considered as high for the necessary pozzolanic reaction [33]. Additionally, the LS in the present study had a weathering index of more than 2.0, which identified it as fersiallitic tropical soil based on the silica to sesquioxide ratio [34]. The scanning electron microscopy (SEM) image in Figure 2a shows small particles in clusters patterns.

Table 2. Chemical compositions of the LS, BA, and HC.

Materials	Chemical Composing (%)											LOI
	SiO_2	Al_2O_3	Fe_2O_3	CaO	MgO	K_2O	SO_3	T_iO_2	Na_2O	P_2O_5	Other	
LS	59.79	20.59	8.07	0.04	1.48	3.05	0.07	0.87	0.03	0.12	0.33	5.56
BA	61.73	8.57	5.32	11.4	1.77	5.02	0.17	0.71	0.14	1.17	0.46	3.54
HC	15.12	3.49	2.98	64.99	1.29	0.46	2.81	0.27	0.11	0.06	0.23	8.19

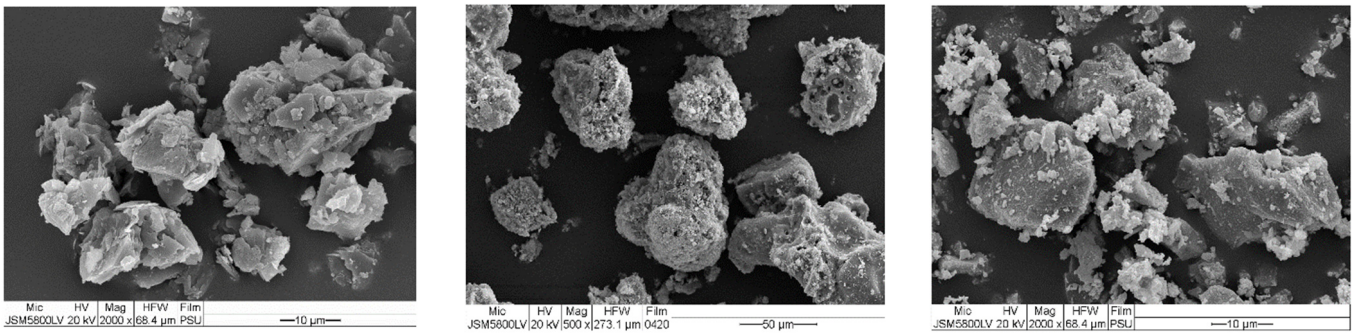

(**a**) (**b**) (**c**)

Figure 2. SEM images: (**a**) lateritic soil; (**b**) biomass bottom ash; (**c**) hydraulic cement.

2.1.2. Biomass Bottom Ash

In this study, the biomass bottom ash (BA) was a by-product of the Para rubber wood combustion from manufacturers of the wood substitute products, which was obtained from Panel Plus Co., Ltd., situated in the Hat Yai Sub-district, in Songkhla Province. The physical and chemical properties of the BA are shown in Tables 1 and 2, respectively. As seen in Table 1, BA has a specific gravity is 2.405, and the D_{50} was 1.60 mm. BA is a non-plastic material and is classified as a poorly graded sand (SP) according to the USCS method. The grain size distribution curve of the BA is depicted in Figure 1. The morphology of the BA in Figure 2b is that of relatively porous particles and rough textures. The XRF analysis (Table 2) showed three major components (SiO_2, Al_2O_3, and Fe_2O_3) which made up 75.62% of the BA, which is more than 70%. Therefore, the BA could be classified as a pozzolanic material Class F based on the ASTM C618 standard [35].

2.1.3. Hydraulic Cement

The Hydraulic Cement (HC) used in this study was from INSEE Petch Plus, which is a general use (GU) type according to the Thailand Industrial Standard (TIS 2594-2013) [36]. The chemical composition (Table 2) revealed the presence of calcium oxide (CaO), which was approximately 65%, and acted as the dominant mineral in the HC. The SEM image (Figure 2c) depicts irregular shapes with sharp corners.

2.2. Sample Preparation and Testing

In this study, the specimen was categorized into two groups, namely, uncemented and cement-stabilized soil (CSS) specimens. The LS was partially replaced with BA at proportions of 0, 40, 60, 80, and 100%. For the CSS specimen, the HC contents of 3, 5, and 7% by weight of the dry soil aggregate (LS + BA) were mixed with a soil aggregate sample. Gradation analysis of the LS blended BA (Figure 1) met the criteria set by the DOH. In Figure 1, the letters S and B refer to amounts of lateritic samples of soil and bottom ash, respectively. For example, S60B40 denotes the mix with 60% LS + 40% BA. Laboratory tests, including compaction tests, the California bearing ratio (CBR) test, and the unconfined compression (UC) test, were conducted to determine the geotechnical characteristics of the mixtures. The details of the testing program are summarized in Table 3.

Table 3. Testing program.

Testing	LS:BA Proportions	Cement Content (%)	Water Content (%)	Curing Time (days)	Remark
Compaction	100:0, 60:40, 40:60, 20:80, 0:100	0	-	-	Uncemented specimens
	60:40, 40:60, 20:80, 0:100	3, 5, 7	-	-	CSS specimens
Soaked CBR	100:0, 60:40, 40:60, 20:80, 0:100	0	OMC	4	Uncemented specimens
UC test	60:40, 40:60, 20:80, 0:100	3, 5, 7	OMC	7, 14, 28	CSS specimens

2.2.1. Compaction and CBR Tests

The modified Proctor test according to ASTM D 1557 [37] was performed to determine the maximum dry unit weight (γ_{dmax}) and optimum moisture content (OMC) for both the uncemented and CSS specimens. In this study, the soaked CBR test according to ASTM D 1883 [38] was conducted only on the uncemented specimen to determine the CBR value for evaluating it as a civil infrastructure material.

2.2.2. Unconfined Compression (UC) Test

The UC test was performed for the CSS specimens according to the specification of the Department of Highways (DOH) of Thailand [32]. The LS and BA samples were passed through a 4.75 mm sieve, and then dried in an oven for 24 h before blending with the HC. They were then mixed with water at an OMC obtained from the compaction test. For each mixture, three replicate specimens were prepared with a diameter of 50.2 mm and a height of 102 mm. Then they were compacted in the cylindrical split mold via a ram of 4.50 kg, with a 200 mm drop length across three layers (21 blows/layer). Each layer reached the specified modified Proctor energy values. After the molding process, the stabilized specimen was carefully extracted from the mold and then wrapped in a plastic bag. It was stored in a humidity chamber at a constant temperature (25 $\pm$ 2 °C). After achieving the specified curing time, the CSS specimens were soaked in water for 2 h, and then the compression test with a compression machine under the constant loading rate with fixed a vertical displacement of 1 mm/min was carried out [32]. The UC tests were conducted for three specimens, and an average value was reported. The secant Young's modulus (E_{50}) was determined from the UC tests to analyze the stiffness of the mix.

2.2.3. Leachate Test

The major concern when stabilizing industrial waste materials (i.e., fly ash, bottom ash) is the leachate's characteristics [13]. Bottom ash contains some harmful chemicals, including heavy metals, which are rapidly leachable. In this study, both uncemented and CSS mixes were compacted in the permeability mold and then kept for curing in a humidity chamber at 25 $\pm$ 2 °C for 7 days. The water outflow from the permeability mold was collected in sampling bottles for leachate analysis.

2.3. Pavement Design

The mechanistic–empirical (M–E) design method is based on material mechanics and relates to an input, such as wheel load, and an output or pavement response, such as stress or strain. Laboratory tests and field performance data are used to predict distress using these response values. As theory alone does not prove sufficient for designing realistic pavements, reliance on the observed performance was required [39]. In this study, stress-strain analysis was performed using the KENLAYER computer program, which is based on the multi-layer elastic theory. The design procedure and input parameters for this analysis are illustrated as follows.

(i) Assigning the number of layers and the thickness of each layer based on the Thailand DOH. The four-layer systems (Figure 3) consisted of a hot mix asphalt (HMA) surface course, base course, subbase course, and natural subgrade.

(ii) Assigning the traffic load condition of a single axle with a dual tire, standard axle load (80 kN), and contact pressure of 690 kPa.
(iii) Pavement materials assumed linear elastic behavior for all layers. The Poisson's ratio (ν) and resilient modulus (MR) were varied depending on specific layers. Determination of the MR values for the stabilized subbase material used the empirical correlation of the unconfined compressive strengths (qu) obtained from this experiment's tests.
(iv) The pavement response analysis to evaluate the benefits of using the CSS as road pavement materials were documented.

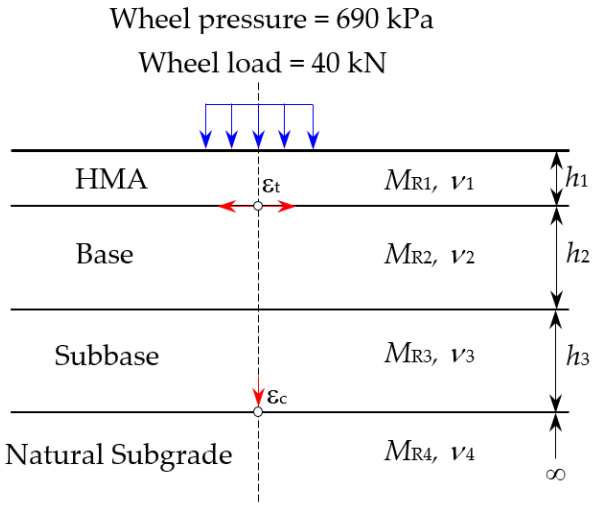

Figure 3. Pavement configuration.

The resilient modulus (M_R) value, which characterizes the mechanical responses of pavement materials, is required as an input parameter in pavement structural design. The M_R test, on the other hand, typically necessitates a significant amount of time and expertise to be carried out correctly [40]. As a result, each test can be costly, and can add significantly to the cost of a highway project. AASHTO [41] recognized the practical issues associated with determining M_R and offers a three-level hierarchical approach: laboratory measurement, empirical correlation with soil properties, and the use of a default value based on soil types for levels 1, 2, and 3, respectively. According to the literature, the q_u value for stabilized soil can be used to predict the M_R, and this method was used in this study. The M_R equations for each material's layers are illustrated in the following equations:

(a) For untreated soil
- For fine-grained soils with *CBR* less than or equal to 10% [42]

$$M_R = 10CBR \quad (1)$$

- For *CBR* > 10% [43]

$$M_R = 17.6CBR^{0.64} \quad (2)$$

(b) For treated soil [44]

$$M_R = 149q_u \quad (3)$$

(c) For HMA, the M_R value presented by Saglik and Gungor [45], which is a simplified Witczak's dynamic modulus equation, was adopted. The experimental results from the study of Lukjan et al., 2022 [46] were used for assessing the M_R values of the hot mix asphalt concrete (HMA) pavement:

$$M_R = 3.75 + 0.029P_{200} - 0.00177[P_{200}]^2 - 0.0028R_4 - 0.058V_a - 0.8[V_b/(V_b + V_a)] + [A/B] \quad (4)$$

$$A = 3.87 - 0.0021R_4 + 0.004R_{3/8} - 1.7 \times 10^{-5}\,[R_{3/8}]^2 + 0.0055R_{3/4} \quad (5)$$

$$B = 1 + e^{-2.56 + 0.89 \log(pen) \; - \; 0.0015[\log(pen)]^2} \quad (6)$$

where M_R = resilient modulus (kPa), q_u = unconfined compressive strength (kPa), V_a = air void (%),V_b = effective asphalt content (%), P_{200} = passing No.200 sieve (%), R_4 = retained No.4 sieve (%), $R_{3/8}$ = retained No.3/8 sieve (%), $R_{3/4}$ = retained No.3/4 sieve (%), and *pen* = penetration of asphalt cement.

2.4. Performance Analysis

The failure patterns of the flexible pavement system generally consist of fatigue cracking and rutting deformation. Fatigue cracking is due to the excessive horizontal tensile strain (ε_t) at the bottom of the surface course, while the occurrence of vertical compressive strain (ε_c) at the top of the subgrade layer causes the rutting deformation. A mechanistic–empirical pavement design, known as a transfer function, was performed in this study to evaluate the overall performance of the pavement [39]. Fatigue and rutting models of the pavement were adopted to evaluate the benefits of the CSS in terms of its traffic benefits ratio (*TBR*). The *TBR* values were defined through the extension in the service life of the pavement system [47] when the CSS was used as the subbase course material.

To predict the life of the pavement, the number of allowable loads before the pavement structure's failure occurs must be determined. For the fatigue model, the desired equation of the Minnesota Department of Transportation [48] was adopted to calculate the allowable number of load repetitions (N_f):

$$N_f = 2.83 \times 10^{-6} \, (\varepsilon_t)^{-3.21} \quad (7)$$

For the rutting model, the allowable numbers of load repetitions (N_r) to produce a rut depth less than 10.2 mm presented by the Transport and Road Research Laboratory (TRRL) [43] with a reliability of 85% was adopted:

$$N_r = 6.18 \times 10^{-8} \, (\varepsilon_c)^{-3.95} \quad (8)$$

Thus, the *TBR* values can be calculated using Equations (9) and (10):

$$TBR_f = (\varepsilon_{tu} / \varepsilon_{ts})^{-3.21} \quad (9)$$

$$TBR_r = (\varepsilon_{cu} / \varepsilon_{cs})^{-3.95} \quad (10)$$

where TBR_f and TBR_r are the traffic benefit ratios corresponding to the N_f and N_r values, respectively; u and s denote unstabilized and stabilized subbase course, respectively.

3. Results

3.1. Compaction and CBR Characteristics

Figure 4 shows the typical compaction curves of the CSS specimens at a different BA and cement content. The compaction curves the γ_{dmax} and OMC for pure lateritic soil (LS) were 18.8 kN/m^3 and 14.4%, respectively. Overall, all compaction curves of CSS specimens were lower than that of LS. As observed in Figure 4a–c, CSS specimens depicted a reduction in the γ_{dmax} values with the increase in the BA content. For example in Figure 4b, the γ_{dmax} decreased from 18.8 kN/m^3 to 18.0, 17.42, 17.0, and 15.48 kN/m^3 after replacement by BA of 40, 60, 80, and 100%, respectively. This decrease in the γ_{dmax} is related to the increase in the OMC of the mixtures, which describes that the LS treated with BA and cement specimens require a higher water content to reach the γ_{dmax}, compared to pure LS. The increase in the OMC was attributed to the replacement of coarse grains by the BA, which had a higher adsorption capacity than the LS [49]. The reduction in the γ_{dmax} was due to the fact that the BA had a specific gravity lower than that of the LS.

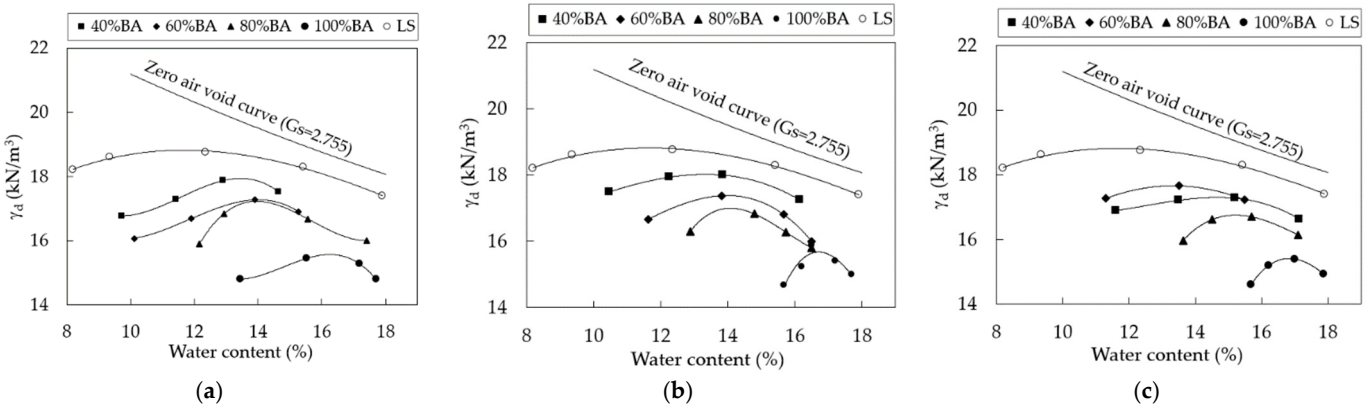

Figure 4. Compaction curves of the CSS specimens: (**a**) cement = 3%; (**b**) cement = 5%; (**c**) cement = 7%.

Figure 5 shows the CBR values of uncemented specimens after 4 days of soaking. The CBR value of the untreated LS was 4%, and this increased to 95, 110, 118, or 85% after blending with the BA at 40, 60, 80, or 100%, respectively. The XRD patterns of the uncemented (80% BA replacement) specimens are depicted in Figure 6a. As seen in Figure 6a, the main component of the specimen was quartz (SiO_2) in a crystalline form. Kaolinite is a clay mineral, and quartz and calcite are non-clay minerals [9]. Therefore, an increase in the CBR value can be explained by the presence of calcium carbonate (CaO) in the BA, which affected the chemical reactions between the CaO and CO_2 in the calcite form, including the pozzolanic reaction, which contributed to the high CBR value, which was confirmed by the XRD graphs in Figure 6a.

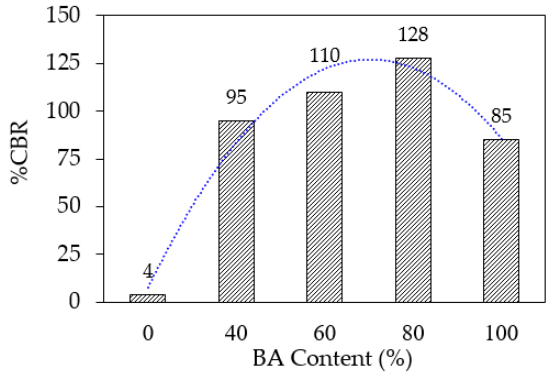

Figure 5. Soaked CBR values of the uncemented specimens.

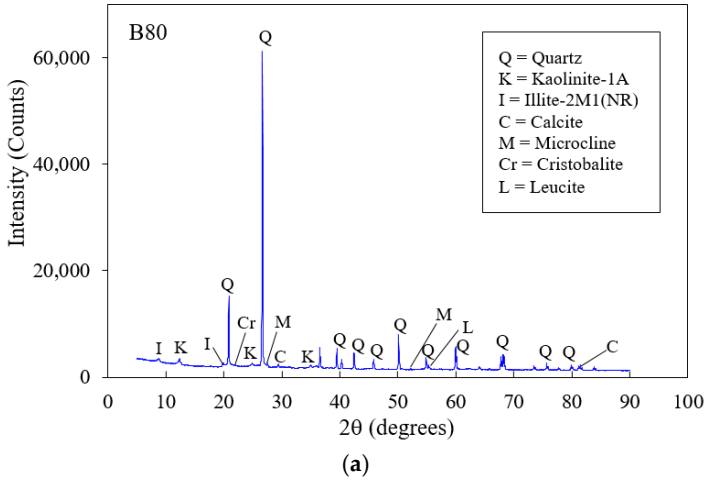

Figure 6. *Cont.*

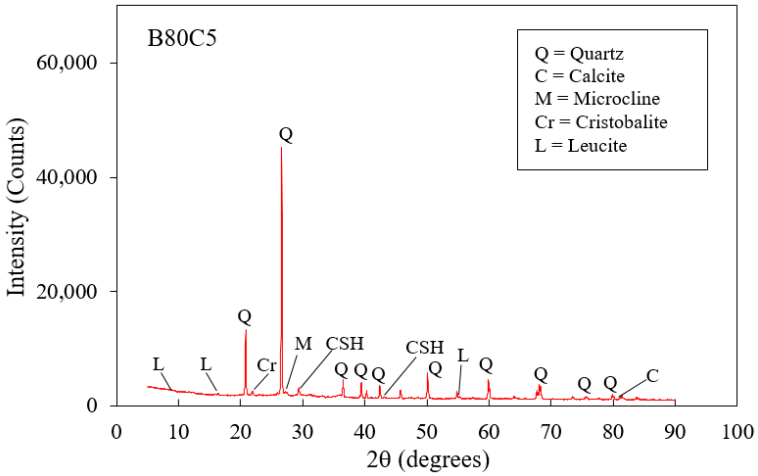

(**b**)

Figure 6. X-ray diffraction patterns: (**a**) B80; (**b**) B80C5.

3.2. Effects of BA and HC Contents on Strength

The mean values of the q_u and E_{50} obtained from the UC test for the CSS specimens are summarized in Table 4. The letters B and C refer to the dosages of the biomass bottom ash and cement, respectively. For example, B40C3 denotes the mixture with the replacement of LS by 40% BA, and is stabilized with 3% HC. Figure 7 depicts the variation in q_u values and BA replacement contents for CSS specimens after 7 days of curing time. The minimum q_u value for the soil–cement subbase at 7 days, as specified by the DOH of Thailand [32], is 689 kPa, as shown by the dashed line. Figure 7 shows that, with the exception of the specimen containing 100% BA and 3% cement, the majority of the specimens met the DOH specifications' minimum values. The strength of all specimens with varying cement content followed a similar pattern, with an increasing trend with increasing cement content. When 40 and 60% BA content were added to specimens stabilized with 3% cement and 7% cement, the q_u tended to increase. Beyond 60% BA addition, a downward trend in the q_u was observed. While the specimens were stabilized at 5% cement, the q_u increased as the BA content increased from 40 to 80%. The q_u decreased as the BA content exceeded 80%. Figure 8 shows the relationship between the q_u of the CSS specimens corresponding to curing times of 7, 14, and 28 days, with the only notable difference being in the cement content. As observed, the q_u values of all CSS specimens increased progressively and logarithmically with the curing time. This trend was consistent with the previous investigation [12,50,51].

Table 4. q_u and E_{50} of the CSS specimens with different curing times.

Specimens	BA Content (%)	Cement Content (%)	q_u (kPa)			E_{50} (kPa)		
			Curing Time (Days)			Curing Time (Days)		
			7	14	28	7	14	28
B0C0	0	0	482	482	482	482	482	482
B40C3	40	3	774	1294	1522	77,400	92,429	76,100
B60C3	60	3	848	1602	1666	32,615	89,000	104,125
B80C3	80	3	753	839	1290	37,650	59,929	80,625
B100C3	100	3	361	459	485	22,563	25,500	40,417
B40C5	40	5	987	1933	2136	82,250	113,706	178,000
B60C5	60	5	932	1823	2299	77,667	151,917	164,214
B80C5	80	5	1374	2332	2726	114,500	233,200	340,750
B100C5	100	5	883	1600	1722	48,938	160,000	86,100
B40C7	40	7	1947	2556	2647	121,688	182,571	132,350

Table 4. *Cont.*

Specimens	BA Content (%)	Cement Content (%)	q_u (kPa)			E_{50} (kPa)		
			Curing Time (Days)			Curing Time (Days)		
			7	14	28	7	14	28
B60C7	60	7	2284	2731	2874	207,000	227,583	287,400
B80C7	80	7	2511	3350	3477	251,100	335,000	347,700
B100C7	100	7	1620	1818	1916	198,417	139,846	95,800

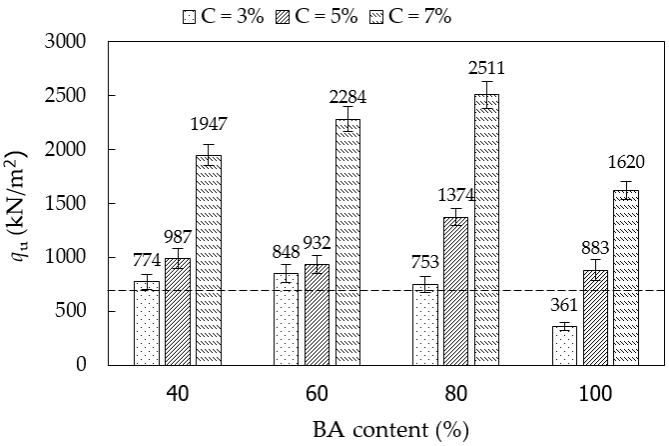

Figure 7. The q_u of CSS specimens for different BA and cement contents at 7 days of curing time.

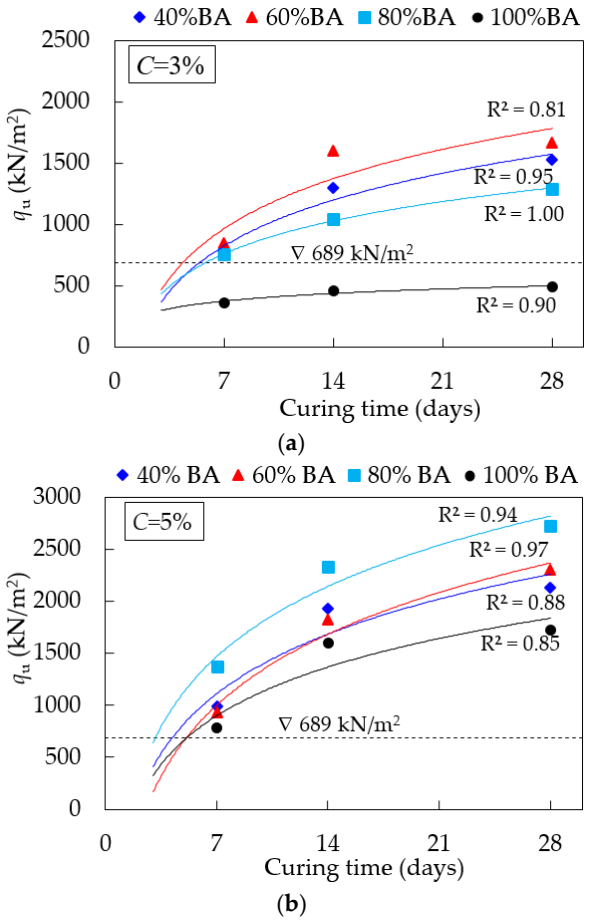

Figure 8. *Cont.*

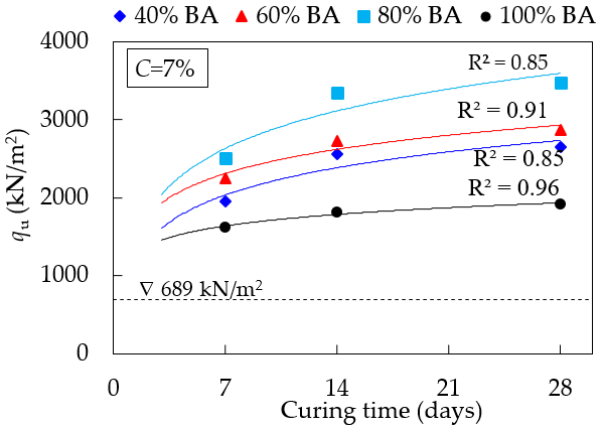

(**c**)

Figure 8. Strength development with the curing time of the CSS: (**a**) cement = 3%; (**b**) cement = 5%; (**c**) cement = 7%.

3.3. Leaching Analysis

The concentrations of the heavy metals obtained from the analysis with an Inductively Coupled Plasma-Optical Emission Spectrometer, Avio500, USA, is presented in Table 5. In this study, the selected samples from pure BA (solid sample) and from the leaching tests were examined. The leachate samples were collected from the effluent flowing out of the permeability test, comprising both the uncemented (i.e., B100, S20B80) and cemented (i.e., B80C5) specimens. For the pure BA, As, Cr, Cu, Ni, and Zn were detected, but Cd and Pb were not detected. According to the allowable limits of the soil's quality standard requirements [52], the concentrations of As and Cr were higher than the allowable limits. For the leachate sample, As, Cd, and Pb were not detected. The concentrations of Cu and Zn from the sample of B100 and S20B80 were below the allowable limits of the groundwater quality standards [53,54]. However, the concentration of Cr was still higher than the allowable limits. This indicated that BA as a road material without the solidification/stabilization (S/S) technique may be unsuitable due to its negative environmental impact.

Table 5. Heavy metal concentrations.

	From Solid Sample		From Leachate Sample				
	B100 (mg/kg)	**Allowable Limits (mg/kg) [52]**	**B100 (ppm)**	**B80C0 (ppm)**	**B80C5 (ppm)**	**Allowable Limits (ppm) [53]/[54]**	**Threshold Limit (ppm) [53]/[54]**
Arsenic (As)	14.80	6	ND	ND	ND	0.01/0.01	1.00/1.00
Cadmium (Cd)	ND	67	ND	ND	ND	0.003/0.005	0.30/0.50
Chromium (Cr)	82.86	17.5	0.065	0.052	0.0225	0.05/0.10	5.00/10.00
Copper (Cu)	16.60	2920	0.102	0.081	0.0731	1.00/1.00	100.00/100.00
Nickel (Ni)	16.64	436.5	0.008	0.006	0.0032	0.02/-	2.00/-
Lead (Pb)	ND	400	ND	ND	ND	0.01/0.015	1.00/1.50
Zinc (Zn)	32.02	-	0.017	0.016	0.0105	5.00/5.00	500.00/500.00

Note: ND = not detected.

According to the US EPA, a material was considered hazardous waste if any detected heavy metal occurs at concentrations greater than 100 times the drinking water standard [55]. As observed in Table 5, the heavy metal concentrations of specimen B80C5 demonstrated that all parameters were within the allowable limit and threshold limit, which can confirm the safe utilization of BA as subbase material. This implied that the solubilities of silica, alumina, and clay minerals in LS are available for the reaction with calcium from cement and/or BA to form the cementitious hydrates, CAH and CSH. This contributed not only to the increased strength and reduced swell of the treated soil, but also to heavy metal immobilization via surface adsorption inclusion, and physical entrapment [56].

3.4. Pavement Design and Analysis

The stress-strain response results from the KENPAVE [39] were analyzed to investigate the overall performance by using the CSS as a subbase course. According to the strength and leaching criteria, B80C5 was selected as a suitable mixture and was subjected to the M–E pavement design. To compare the simulation results between unstabilized and stabilized subbase material, the thickness (h) of the HMA and the base course layer was considered constant, and the thickness of the subbase layer was varied by 200, 175, 150, and 125 mm, respectively.

The material's properties as an input parameter model are shown in Table 6. For unstabilized subbase (Conventional material), the pavement structure had a 100 mm HMA surface course, 200 mm crushed stone base course, 200 mm granular subbase course, and an infinite extent of natural subgrade. The stabilized subbase had the same load condition as that of the unstabilized sample, but that was replaced with the CSS material's property. Considering the input parameters of the stabilized subbase layer in Table 6, the q_u value (2.70 Mpa) was obtained from the strength after 28 days for the B80C5 specimen. It also satisfied the minimum requirement for medium to high volume roads of the stabilized subbase (i.e., 2.0 MPa), as per the Austroads specification [57]. Thus, the M_R value for the soil–cement subbase obtained from Equation (3) was 400 MPa.

Table 6. Input model parameters.

Model Layer	Pavement Layer	h(cm)	Conventional Materials			Stabilized-Subbase Materials			
			M_R (MPa)	ν	CBR (%)	M_R (MPa)	ν	CBR (%)	q_u (MPa)
1	HMA	10	3000	0.35	-	3,000	0.35	-	-
2	Base	20	300	0.35	85	300	0.35	85	-
3	Subbase	20, 17.5, 15, 12.5	150	0.35	30	400	0.30	-	2.70
4	Subgrade	∞	50	0.40	5	50	0.40	5	-

Table 7 presents the M–E response at any location, including the surface deflection (Δ_z); the tensile strain (ε_t) at the bottom of the surface; and the vertical compressive strain (ε_c) at the top of the subgrade. As observed in Table 7, all Δ_z, ε_t, and ε_c values of the stabilized subbase had lower values than those of the conventional pavement, indicating the influences of the stabilized subbase. The value of N_f was more than N_r for the unstabilized subbase, which illustrates the critical number of repetitions (N_{cr}) that occurred with rutting failures. On the other hand, the N_f became less than that of the N_r for the thicknesses of 200 and 175 mm for the stabilized subbase, which indicates that the N_{cr} occurred with fatigue failures. This indicates that it is the effect of using the stabilized layer. However, when the thickness of the subbase was reduced to 150 or 125 mm, the N_{cr} became an N_r again.

Table 7. Results of mechanistic–empirical design.

Subbase Course	Subbase Thicks, mm	Constant HMA and Base Course						
		Δ_z (mm)	ε_t ($\times 10^{-4}$)	ε_c ($\times 10^{-4}$)	N_f ($\times 10^6$)	N_r ($\times 10^6$)	TBR_f	TBR_r
Unstabilized	200	0.55	2.41	4.44	1.16	1.08	1.00	1.00
Stabilized	200	0.48	2.24	3.63	1.47	2.41	1.27	2.23
	175	0.49	2.26	3.90	1.44	1.81	1.24	1.67
	150	0.51	2.25	4.20	1.39	1.34	1.20	1.23
	125	0.60	2.35	5.31	1.25	0.53	1.08	0.49

4. Discussions

4.1. Strength Development and Stiffness

To analyze the effect of cement and BA content on the strength development for the CSS specimens, the q_u value at 28 days of curing time and cement content relationship is presented in Figure 9. As observed, the strength increment was logarithm, and increased

in trend with the increase in cement content. The q_u value of the specimen with 80% BA showed a remarkable strength development versus other samples. Its strength increased by 3, 6, and 7 times for 3, 5, and 7% cement-treated samples, respectively, when compared with the untreated soil sample. Theoretically, the strength development of the cement-treated soil mainly depends on the hydration reaction and the pozzolanic reaction for short-term and long-term stages, respectively. Calcium-based stabilizers (e.g., cement) play an important role in producing calcium silicate hydrate (CSH), calcium aluminate hydrate (CAH), and calcium aluminosilicate hydrate (CASH) gels [9,12,44]. The main component of the specimen was quartz (SiO_2) in crystal form, as shown by the XRD patterns of the CSS (B80C5) specimens after 28 days of curing time in Figure 6b. When the sample was treated with cement, the XRD results showed a reduction in the amount of crystals (i.e., compared with Figure 6a). This can be explained by the class F pozzolanic material not readily exhibiting self-cementing characteristics, and pozzolanic reactions are initiated upon cement addition, leading to the formation of CAH and CSH cementitious products. Overall, the CSH products are induced by the rapid hydration reaction between CaO in the HC and SiO_2 in the LS and BA, which increases the q_u. The results agreed quite well with the previous studies found by [58] for cement and biomass ash-treated soil.

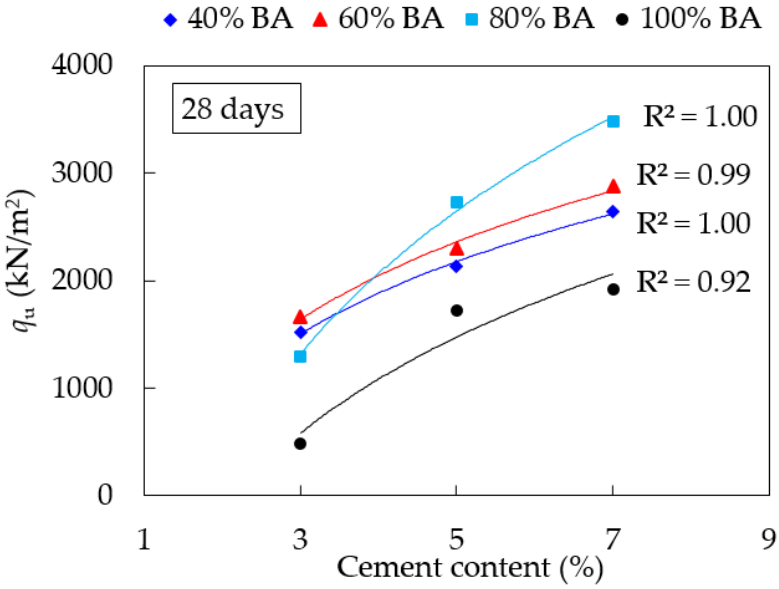

Figure 9. Relationship between q_u and cement content at 28 days of curing time.

The secant modulus (E_{50}) obtained from the stress-strain curve was used to explain the stiffness of the CSS specimens. Figure 10 shows the relationship between the E_{50} and q_u values of the CSS specimens (i.e., 3, 5, and 7% cement contents) at 7, 14, and 28 days of the curing time. Regarding Figure 10, the E_{50} increased linearly with an increase in the q_u value, which was varied from $40q_u$ to $125q_u$ (i.e., red line in Figure 10) with the best fitting line of $84q_u$ and the R^2 of 0.872. It can be seen that the obtained E_{50}-q_u correlation from this study was consistent with the previous studies. For example, it was slightly lower than $106.82q_u$ for the cemented-lateritic soil in Malaysia which was presented by Wahab et al. [12]. Similar results were reported by Al-Jabban et al. [59] for the cement-treated sandy clayey silt in Sweden (i.e., $85q_u$) and Yin [60] for the cement-treated Hong Kong marine deposit (i.e., $89q_u$). Therefore, it is suggested that the relationship between E_{50} and q_u obtained from this study can be reliable in utilization in road pavement applications.

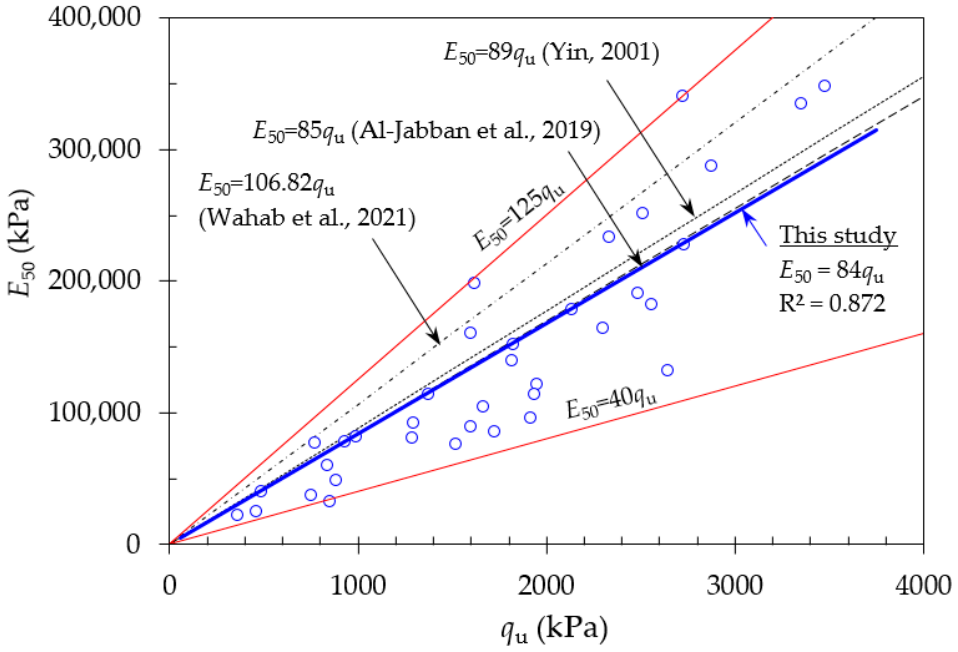

Figure 10. The relationship between the E_{50} and q_u compared with the previous study.

4.2. Benefit of BA for Subbase Stabilization

This study demonstrates the benefit of using BA as an aggregate material for flexible pavement. It was discovered that low-quality LS treated with BA and cement increased the q_u value and met the DOH's minimum requirement for the soil–cement subbase for all mixtures. This could demonstrate that using waste BA at a minimum of 40% (by weight of mix) as an aggregate with a cement content of 3 to 7% is feasible. As previously discussed, cementitious products play an important role in the strength development of CSS admixtures. The pore size reduction effect is another reason to support the positive results of CSS containing BA. This explains how cement stabilization improves soil structure by increasing inter-cluster cementation bonding and decreasing the pore space of the mix [61], resulting in improved pavement performance. Considering the *TBR* values as presented in Table 7, using the CSS as the subbase material could improve the life of the pavement by 1.27, 1.24, and 1.23 times for the subbase thicknesses of 200, 175, and 150 mm, respectively, compared with the conventional pavement system. For the subbase thicknesses of 125 mm, the *TBR*r value was reduced to 0.49, indicating that the stabilized subbase thickness should not be lower than 150 mm. According to the M–E method analysis presented in this study, the use of CSS containing BA as soil aggregate can reduce distress in flexible pavement. The current investigation, however, did not include any long-term durability studies. Concerning the contaminant issues, the heavy metal concentration of the proposed CSS mix confirmed that the leachate of heavy metal is below allowable limits acceptable for contaminants flowing into groundwater. It can therefore, be suggested that the knowledge gained will be critical for future research on similar waste BA materials in other areas.

5. Conclusions

The following conclusions can be drawn from the present study:

1. The soaked CBR values of the poor-quality LS were improved as a result of blending with BA, which met the requirement for subbase material in the Thailand highway specifications. However, the LS mixed with BA was still unsuitable for use as road material, because the Cr concentration still exceeded the national allowable limits for drinking water.
2. The results of the UC test on the CSS specimens indicated that it had a significant strength improvement, which satisfied the minimum requirement for soil–cement

subbase course. To maximize the utilization of the BA, the blend of the LS with 80% BA and cement-stabilized with 5% is suggested for applications in the subbase layer of pavement. It had remarkable results in terms of geotechnical engineering properties and has no environmental impact.

3. The results of the M–E approach pavement analysis indicated that using the CSS presented in this study as a soil–cement subbase layer would reduce the layer thickness by a maximum of 25%; extend the service life of the pavement; and extend the fatigue life and the rutting life by 1.20–1.27 times and 1.23–2.23 times respectively.
4. The outcomes of this research could be helpful for the development of new mixtures for future use of recycled biomass bottom ash in pavement applications.

Author Contributions: Conceptualization, A.I. and A.L.; methodology, A.L.; software, A.L.; validation, A.I., P.P. and A.L.; formal analysis, A.I., P.P. and A.L.; investigation, A.I. and A.L.; resources, A.L.; data curation, A.I.; writing—original draft preparation, A.I. and A.L.; writing—review and editing, P.P. and A.L.; visualization, A.L.; supervision, P.P. and A.L.; project administration, A.L.; funding acquisition, A.L. All authors have read and agreed to the published version of the manuscript.

Funding: This research was funded by the Rajamangala University of Technology Srivijaya, Thailand.

Institutional Review Board Statement: Not applicable.

Informed Consent Statement: Not applicable.

Data Availability Statement: The data presented in this study are available on request from the corresponding author.

Acknowledgments: The authors gratefully acknowledge the support of the Department of Civil Engineering, Faculty of Engineering, Rajamangala University of Technology Srivijaya.

Conflicts of Interest: The authors declare no conflict of interest.

References

1. Office of the National Economic and Social Development Board. National Strategy (2018–2037). 2018. Available online: https://sto.go.th/en/about/policy/20-year-strategic-plan (accessed on 8 April 2022).
2. Rashid, A.S.A.; Latifi, N.; Meehan, C.L.; Manahiloh, K.N. Sustainable improvement of tropical residual soil using an environmentally friendly additive. *Geotech. Geol. Eng.* **2017**, *35*, 2613–2623. [CrossRef]
3. Fredlund, D.G.; Rahardjo, H. *Soil Mechanics for Unsaturated Soils*; John Wiley&Sons, Inc.: New York, NY, USA, 1993.
4. Koppejan, J.; Van Loo, S. *The Handbook of Biomass Combustion and Co-Firing*; Routledge: London, UK, 2012.
5. Lu, Y.; Tian, A.; Zhang, J.; Tang, Y.; Shi, P.; Tang, Q.; Huang, Y. Physical and chemical properties, pretreatment, and recycling of municipal solid waste incineration fly ash and bottom ash for highway engineering: A literature review. *Adv. Civ. Eng.* **2020**, *2020*, 8886134. [CrossRef]
6. López, E.L.; Vega-Zamanillo, A.; Pérez, M.A.C.; Hernández-Sanz, A. Bearing capacity of bottom ash and its mixture with soils. *Soil Found.* **2015**, *55*, 529–535. [CrossRef]
7. Cabrera, M.; Galvín, A.P.; Agrela, F.; Carvajal, M.D.; Ayuso, J. Characterisation and technical feasibility of using biomass bottom ash for civil infrastructures. *Constr. Build. Mater.* **2014**, *58*, 234–244. [CrossRef]
8. Paine, K.A.; Dhir, R.K.; Doran, V.P.A. Incinerator bottom ash: Engineering and environmental properties as a cement bound paving material. *Int. J. Pavement Eng.* **2002**, *3*, 43–52. [CrossRef]
9. Jaritngam, S.; Somchainuek, O.; Taneerananon, P. An investigation of lateritic soil cement for sustainable pavements. *Indian J. Sci. Technol.* **2012**, *5*, 2603–2606. [CrossRef]
10. Berra, M.; Mangialardi, T.; Paolini, A.E. Reuse of woody biomass fly ash in cement-based materials. *Constr. Build. Mater.* **2015**, *76*, 286–296. [CrossRef]
11. Donrak, J.; Hoy, M.; Horpibulsuk, S.; Arulrajah, A.; Mirzababaei, M.; Rashid, A.S.A. Environmental assessment of cement stabilized marginal lateritic soil/melamine debris blends for pavement applications. *Environ. Geotech.* **2019**, 1–7. [CrossRef]
12. Wahab, N.A.; Roshan, M.J.; Rashid, A.S.A.; Hezmi, M.A.; Jusoh, S.N.; Norsyahariati, N.D.N.; Tamassoki, S. Strength and durability of cement-treated lateritic soil. *Sustainability.* **2021**, *13*, 6430. [CrossRef]
13. Ghosh, A.; Subbarao, C. Hydraulic conductivity and leachate characteristics of stabilized fly ash. *J Env. Eng.* **1998**, *124*, 812–820. [CrossRef]
14. Bruder-Hubscher, V.; Lagarde, F.; Leroy, M.J.F.; Coughanowr, C.; Enguehard, F. Utilisation of bottom ash in road construction: Evaluation of the environmental impact. *Waste Manag. Res.* **2001**, *19*, 545–556. [CrossRef]
15. Yoon, S.; Balunaini, U.; Yildirim, I.Z.; Prezzi, M.; Siddiki, N.Z.J. Construction of an embankment with a fly and bottom ash mixture: Field performance study. *Mater. Civ. Eng.* **2009**, *21*, 271–278. [CrossRef]

16. Dabo, D.; Badreddine, R.; De Windt, L.; Drouadaine, I. Ten-year chemical evolution of leachate and municipal solid waste incineration bottom ash used in a test site. *J. Hazard. Mater.* **2009**, *172*, 904–913. [CrossRef]
17. del Valle-Zermeño, R.; Formosa, J.; Prieto, M.; Nadal, R.; Niubó, M.; Chimenos, J.M. Pilot-scale road subbase made with granular material formulated with MSWI bottom ash and stabilized APC fly ash: Environmental impact assessment. *J. Hazard Mater.* **2014**, *266*, 132–140. [CrossRef]
18. Cabrera, M.; Galvín, A.P.; Agrela, F.; Beltran, M.G.; Ayuso, J. Reduction of leaching impacts by applying biomass bottom ash and recycled mixed aggregates in structural layers of roads. *Materials* **2016**, *9*, 228. [CrossRef]
19. Selvi, P. Fatigue and rutting strain analysis on lime stabilized subgrades to develop a pavement design chart. *Transp. Geotech.* **2015**, *2*, 86–98. [CrossRef]
20. Lekha, B.M.; Goutham, S.; Shankar, A.U.R. Evaluation of lateritic soil stabilized with Arecanut coir for low volume pavements. *Transp. Geotech.* **2015**, *2*, 20–29. [CrossRef]
21. Sahu, V.; Srivastava, A.; Misra, A.K.; Sharma, A.K. Stabilization of fly ash and lime sludge composites: Assessment of its performance as base course material. *Arch. Civ. Mech. Eng.* **2017**, *17*, 475–485. [CrossRef]
22. Anaokar, M.; Mhaiskar, S. Numerical analysis of lime stabilized capping under embankments based on expansive subgrades. *Heliyon* **2019**, *5*, e02473. [CrossRef]
23. Yang, X.; Zhang, Y.; Li, Z. Embankment displacement PLAXIS simulation and microstructure behavior of treated-coal gangue. *Minerals* **2020**, *10*, 218. [CrossRef]
24. Sultan, S.A.; Guo, Z. Evaluating the performance of sustainable perpetual pavement using recycled asphalt pavement in China. *Int. J. Transp. Sci. Technol.* **2016**, *5*, 200–209. [CrossRef]
25. Loulizi, A.; Al-Qadi, I.L.; Elseifi, M. Difference between in situ flexible pavement measured and calculated stresses and strains. *J. Transp. Eng.* **2006**, *132*, 574–579. [CrossRef]
26. Solanki, P.; Zaman, M.; Muraleetharan, K.K.; Timm, D. Evaluation of resilient moduli of pavement layers at an instrumented section on I-35 in Oklahoma. *Road Mater. Pavement Des.* **2009**, *10*, 167–188. [CrossRef]
27. Solanki, P.; Zaman, M. Design of semi-rigid type of flexible pavement. *Int. J. Pavement Res. Technol.* **2017**, *10*, 99–111. [CrossRef]
28. Galvín, A.P.; López-Uceda, A.; Cabrera, M.; Rosales, J.; Ayuso, J. Stabilization of expansive soils with biomass bottom ashes for an eco-efficient construction. *Environ. Sci. Pollut. Res.* **2020**, *28*, 24441–24454. [CrossRef]
29. Barcelo, L.; Kline, J.; Walenta, G.; Gartner, E. Cement and carbon emissions. *Mater. Struct.* **2013**, *47*, 1055–1065. [CrossRef]
30. Tosti, L.; Zomeren, A.V.; Pels, J.R.; Damgaard, A.; Comans, R.N.J. Life cycle assessment of the reuse of fly ash from biomass combustion as secondary cementitious material in cement products. *J. Clean. Prod.* **2020**, *245*, 118937. [CrossRef]
31. Songkhla Province. Songkhla Provincial Development Plan (2018–2022). 2021. Available online: https://www.songkhla.go.th/news_develop_plan (accessed on 8 April 2022). (In Thai)
32. Department of Highways (DOH). *Standard of Soil-Cement Subbase*; DH-S 206/2532; Department of Highways Standard: Bangkok, Thailand, 1989. (In Thai)
33. Horpibulsuk, S.; Phetchuay, C.; Chinkulkijniwat, A.; Cholaphatsorn, A. Strength development in silty clay stabilized with calcium carbide residue and fly ash. *Soils Found.* **2013**, *53*, 477–486. [CrossRef]
34. Fookes, P.G. *Tropical Residual Soils: A Geological Society Engineering Group*; Geological Society of London: London, UK, 1997.
35. ASTM. *Standard Specification for Coal Fly Ash and Raw or Calcined Natural Pozzolan for Use in Concrete*; ASTM C 618; ASTM International: West Conshohocken, PA, USA, 2012.
36. Thai Industrial Standards Institute (TISI). *Hydraulic Cement*; TIS 2594-2013; Industrial Product Standards: Bangkok, Thailand, 2013. (In Thai)
37. ASTM. *Standard Test Methods for Laboratory Compaction Characteristics of Soil Using Modified Effort (56,000 ft-lbf/ft3 (2700 kN-m/m3)*; ASTM D 1557; ASTM International: West Conshohocken, PA, USA, 2017.
38. ASTM. *Standard Test Method for California Bearing Ratio (CBR) of Laboratory-Compacted Soils*; ASTM D 1883; ASTM International: West Conshohocken, PA, USA, 2016.
39. Huang, Y.H. *Pavement Analysis and Design*, 2nd ed.; Prentice Hall Inc.: Hoboken, NJ, USA, 2004.
40. Miller, G.A.; Cerato, A.B.; Snethen, D.R.; Holderby, E.; Boodagh, P. Empirical method for predicting time-dependent strength and resilient modulus of chemically treated soil. *Transp. Geotech.* **2021**, *29*, 100551. [CrossRef]
41. AASHTO. *AASHTO Guide for Design of Pavement Structures*; American Association of State Highway and Transportation Officials (AASHTO): Washington, DC, USA, 2003.
42. Heukelom, W.; Klom, A.J.G. Dynamics Testing as a Means of Controlling Pavement During and After Construction. In Proceeding of the International Conference on the Structure Design of Asphalt Pavement, Ann Arbor, MI, USA, 20–24 August 1962.
43. Powell, W.D.; Potter, J.F.; Mayhew, H.C.; Nunn, M.E. *The Structural Design of Bituminous Roads*; TRRL Report 1132; Transport and Road Research Laboratory (TRRL): Berkshire, UK, 1984.
44. Yoobanpot, N.; Jamsawang, P.; Simarat, P.; Pornkasem, J.; Likitlersuang, S. Sustainable reuse of dredged sediments as pavement materials by cement and fly ash stabilization. *J. Soils Sediments* **2020**, *20*, 3807–3823. [CrossRef]
45. Sağlik, A.; Gungor, G. Resilient modulus of unbound and bituminous bound road materials. In Proceeding of the 5th Eurasphalt & Eurobitume Congress, Istanbul, Turkey, 13–15 June 2012.
46. Lukjan, A.; Iyaruk, A.; Somboon, C. Evaluation on mechanical deterioration of the asphalt mixtures containing waste materials when exposed to corrosion solutions. *Int. J. Eng. Technol. Innov.* **2022**, *12*, 130–144. [CrossRef]

47. Al-Hadidy, A.I.; Yi-qiu, T. Mechanistic approach for polypropylene-modified flexible pavements. *Mater. Des.* **2009**, *30*, 1133–1140. [CrossRef]
48. Timm, D.; Birgisson, B.; Newcomb, D. Development of mechanistic-empirical pavement design in Minnesota. *Transp. Res. Rec.* **1998**, *1629*, 181–188. [CrossRef]
49. Lynn, C.J.; Ghataora, G.S.; Dhir OBE, R.K. Municipal incinerated bottom ash (MIBA) characteristics and potential for use in road pavements. *Int. J. Pavement Res. Technol.* **2017**, *10*, 185–210. [CrossRef]
50. Horpibulsuk, S.; Katkan, W.; Sirilerdwattana, W.; Rachan, R. Strength development in cement stabilized low plasticity and coarse grained soils: Laboratory and field study. *Soils Found.* **2006**, *46*, 351–366. [CrossRef]
51. Yoobanpot, N.; Jamsawang, P. Effect of cement replacement by rice husk ash on soft soil stabilization. *Kasetsart J. (Nat. Sci.)* **2014**, *48*, 323–332.
52. Ministry of Natural Resources and Environment, Thailand. *Soil Quality Standards*; The notification of the national environmental committee: Bangkok, Thailand, 2021. (In Thai)
53. Ministry of Natural Resources and Environment, Thailand. *Groundwater Quality Standards*; The notification of the national environmental committee: Bangkok, Thailand, 2004. (In Thai)
54. US Environmental Protection Agency: US EPA. *National Primary Drinking Water Regulations*; EPA: Washington, DC, USA, 2009.
55. Wartman, J.; Grubb, D.G.; Nasim, A. Select engineering characteristics of crushed glass. *J. Mater. Civ. Eng.* **2004**, *16*, 526–539. [CrossRef]
56. Dermatas, D.; Meng, X. Utilization of fly ash for stabilization/solidification of heavy metal contaminated soils. *Eng. Geol.* **2003**, *70*, 377–394. [CrossRef]
57. Rechard, Y. *The Development and Evaluation of Protocols for the Laboratory Characterisation of Cemented Materials*; Austroads Technical Report, AP-T101/08; Austroads: Sydney, Australia, 2008.
58. Cabrera, M.; Agrela, F.; Ayuso, J.; Galvin, A.P.; Rosales, J. Feasible use of biomass bottom ash in the manufacture of cement treated recycled materials. *Mater. Struct.* **2016**, *49*, 3227–3238. [CrossRef]
59. Al-Jabban, W.; Laue, J.; Knutsson, S.; Al-Ansari, N. A comparative evaluation of cement and by-product petrit T in soil stabilization. *Appl. Sci.* **2019**, *9*, 5238. [CrossRef]
60. Yin, J.-H. Stress-strain-strength characteristics of soft Hong Kong marine deposits without or with cement treatment. *Lowland Technol. Int.* **2001**, *3*, 1–13.
61. Horpibulsuk, S.; Rachan, R.; Chinkulkitnuwat, A.; Raksachon, T. Analysis of strength development in cement-stabilized silty clay from microstructural considerations. *Constr. Build. Mater.* **2010**, *24*, 2011–2021. [CrossRef]